Nitric Oxide–Donating Aspirin Derivatives Suppress Microsatellite Instability in Mismatch Repair–Deficient and Hereditary Nonpolyposis Colorectal Cancer Cells

Michael A. McIlhatton,[1] Jessica Tyler,[1] Susan Burkholder,[2] Josef Ruschoff,[3] Basil Rigas,[4] Levy Kopelovich,[5] and Richard Fishel[1]

[1]Department of Molecular Virology, Immunology, and Medical Genetics, Human Cancer Genetics, The Ohio State University Comprehensive Cancer Center and Medical Center, Columbus, Ohio; [2]Department of Pathology, Anatomy, and Cell Biology, Thomas Jefferson University, Philadelphia, Pennsylvania; [3]Institute of Pathology, Klinikum Kassel, and TARGOS Molecular Pathology GmbH, Kassel, Germany; [4]Division of Cancer Prevention, State University of New York at Stony Brook, Stony Brook, New York; and [5]Division of Cancer Prevention, NIH/NCI/DCP, Bethesda, Maryland

Abstract

Nitric oxide–donating nonsteroidal anti-inflammatory drugs (NO-NSAIDs) are an emergent class of pharmaceutical derivatives with promising utility as cancer chemopreventive agents. Aspirin and sulindac have been shown to be effective in selecting for cells with reduced microsatellite instability (MSI) that is inherent in mismatch repair (MMR)–deficient hereditary nonpolyposis colorectal cancer (HNPCC) cells. The effect of NO-NSAIDs on MSI in MMR-deficient HNPCC cells is unknown. Here, we have examined genetically defined MMR-deficient murine embryo fibroblasts, murine colonocytes, and isogenic human HNPCC tumor cell lines treated with acetylsalicylic acid (aspirin; ASA) and three isomeric derivatives of NO-aspirin (NO-ASA). The MSI profiles were determined and compared with the Bethesda Criteria. We found that the ASA- and NO-ASA–treated MMR-deficient cell lines displayed a dose-dependent suppression of MSI that appeared as early as 8 weeks and gradually increased to include up to 67% of the microsatellite sequences examined after 19 to 20 weeks of continuous treatment. Residual resistance to microsatellite stabilization was largely confined to mononucleotide repeat sequences. Control (MMR-proficient) cells showed no changes in microsatellite status with or without treatment. The relative dose-dependent stabilization selection was: *ortho*-NO-ASA ≈ *para*-NO-ASA > *meta*-NO-ASA ≫ ASA. Moreover, the doses required for stabilization by the *ortho*- and *para*-NO-ASA were 300- to 3,000-fold lower than ASA. These results suggest that NO-ASA derivatives may be more effective at suppressing MSI in MMR-deficient cell lines than ASA and should be considered for chemopreventive trials with HNPCC carriers. [Cancer Res 2007;67(22):10966–75]

Introduction

Nitric oxide–donating nonsteroidal anti-inflammatory drugs (NO-NSAIDs) are an emerging class of compounds that may prove efficacious as chemopreventive agents in the treatment of colorectal and other forms of cancer (1, 2). Several studies have shown that NO-NSAIDs inhibit the growth of a variety of human tumor cell lines 10- to 6,000-fold more potently than their parental counterparts (3–5). NO-aspirin (NO-ASA) derivatives have been reported as the most potent of the NO-NSAIDs studied to date (6, 7). In specific experimental systems, NO-ASAs appear to be at least 100-fold more active than other NO-NSAIDs (3, 5). They may be synthesized as one of three different positional isomers, *ortho*-, *meta*-, or *para*-, depending on where the nitrogen-donating (CH_2ONO_2) group is attached to the benzene spacer (Fig. 1).

The observed pharmacologic superiority of NO-ASA versus ASA has been extended to more physiologically relevant models of tumor formation in rats and mice (8, 9). In both animal models, NO-ASA was more effective than ASA in reducing tumor burden. Recent studies in rats and hamsters have shown that NO-ASA can be administered at levels up to 3,000 ppm without deleterious effects on the animal model (10, 11). Furthermore, a recent clinical study has shown that administration of *meta*-NO-ASA to human subjects for 1 week resulted in minimal gastrointestinal toxicity (12). The potential advantages of incorporating NO-ASA into a chemopreventive regime are immediately obvious: (*a*) retention of the well-documented prophylactic antitumorigenic activity of ASA and (*b*) alleviation/elimination of side effects associated with long-term ASA administration, notably gastrointestinal and renal damage.

DNA mismatch repair (MMR) functions in the repair of postreplication misincorporation errors, mismatches generated during genetic recombination, repair of several DNA damage–specific lesions, as well as apoptotic signaling following extensive genomic damage (for review, see ref. 13). The human MMR proteins function as heterodimers (for review, see ref. 14). The human MutS homologues (MSH) play a fundamental role in mismatch/lesion/structure recognition and include hMSH2-hMSH3, hMSH2-hMSH6, and hMSH4-hMSH5. The human MutL homologues (MLH) appear to transduce the initial MSH recognition to downstream effectors that include hMLH1-hPMS1, hMLH1-hPMS2, and hMLH1-hMLH3. There is compelling evidence that links hMSH2, hMSH6, hMLH1, and hPMS2 with hereditary nonpolyposis colorectal cancer (HNPCC; ref. 15). The remaining MSH and MLH homologues are either unlinked to HNPCC (hMSH3, hMSH4, hMSH5, hPMS1) or remain controversial (hMLH3; ref. 16). Tumor tissues from the vast majority of HNPCC cases associated with MMR defects display microsatellite instability (MSI; ref. 17). MSI is generally considered a convenient marker of the elevated mutation rates (mutator phenotype) associated with MMR defects. It is the mutator phenotype that

Requests for reprints: Richard Fishel, Department of Molecular Virology, Immunology, and Medical Genetics, Human Cancer Genetics, The Ohio State University Comprehensive Cancer Center and Medical Center, 400 West 12th Avenue, Columbus, OH 43026. Phone: 614-292-2484; Fax: 215-503-6739; E-mail: rfishel@osu.edu.

doi:10.1158/0008-5472.CAN-07-2562

Table 1. Estimated IC_{50} in μmol/L for cell lines treated with ASA and NO-ASAs

Drug	Colonocytes		E1A MEFs		HCT116		
	$p53^{-/-}$	$p53^{-/-}Msh2^{-/-}$	$Msh2^{+/+}$	$Msh2^{-/-}$	HCT116	+chr2	+chr3
					$hMLH1^{-/-}$	$hMLH1^{-/-}$	$hMLH1^{+}$
ASA	700	1,400	400	700	760	770	630
ortho-NO-ASA	0.5	0.7	0.3	1.0	0.54	0.54	0.67
meta-NO-ASA	91	148	64.5	83	59	138	151
para-NO-ASA	0.5	0.5	0.1	0.5	0.81	2.29	1.25

NOTE: IC_{50} are for 5 days of treatment.

has been suggested to provide the environment for the accumulation of the multiple mutations that appears to drive tumorigenesis (18).

Our previous work demostrated that ASA and sulindac suppressed the MSI mutator phenotype of several human colon tumor cell lines (19). The mechanism appeared to be via a genetic selection that enhanced apoptosis in cells undergoing MSI. These observations suggested a potential prophylactic treatment for the HNPCC genetic susceptibility. Unfortunately, the toxicity and side effects of prolonged ASA or sulindac treatment significantly reduces enthusiasm for their effective use as chemopreventives.

Here, we have examined isogenic Msh2-deficient murine fibroblast and colonic epithelial cell lines as well as near-isogenic human hMLH1-deficient human colon tumor cell lines to determine the efficacy of the *ortho*-, *meta*-, and *para*-NO-ASA derivatives on the suppression of MSI. We found that all of the NO-ASA positional isomers suppress MSI following 8 to 12 weeks of continuous treatment. These results are consistent with our previous conclusion that ASA aids in the acquisition of a microsatellite-stable (MSS) phenotype via a genetic selection process (19). Because MSI is required to accelerate tumorigenesis in HNPCC and MMR-deficient mice, these results suggest that NO-ASAs may be an important chemopreventive for HNPCC.

Materials and Methods

Cell lines. Murine embryonic fibroblasts (MEFs) were isolated from 12 to 13 dpc embryos using standard methods. Early passage MEFs were immortalized with the adenovirus 12S *E1A* gene using the protocols outlined by McCurrach and Lowe (20). E1A-transformed MEFs were produced from wild-type and $Msh2^{-/-}$ MEFs. Colonocyte cell lines were generated from $p53^{-/-}$ and $p53^{-/-}Msh2^{-/-}$ mice according to Sevignani et al. (21). The HCT116($hMLH1^{-/-}$) cell line was obtained from the American Type Culture Collection. HCT116($hMLH1^{-/-}$) cells complemented with either human chromosome 2 [HCT116($hMLH1^{-/-}$)+chr2($hMLH1^{-}$)], or chromosome 3 [HCT116($hMLH1^{-/-}$)+chr3($hMLH1^{+}$)], were provided by the laboratory of Dr. Richard Boland (Baylor University Medical Center, Dallas, TX; ref. 22). All cell lines were grown in DMEM containing 25 mmol/L of D-glucose, 4 mmol/L of L-glutamine, and 25 mmol/L of HEPES (Life Technologies). The medium was supplemented with 10% (v/v) FCS (Life Technologies) and 50 μg/mL of penicillin/streptomycin.

ASA and NO-ASA reagents. ASA (Sigma) was dissolved in DMSO to give a stock solution of 2 mol/L. The NO-donating derivatives of ASA [2-(acetyloxy)benzoic acid 2-[(nitrooxy)methyl]phenyl ester; NCX-4060] (*ortho*-NO-ASA) and [2-(acetyloxy)benzoic acid 4-[(nitrooxy)methyl]phenyl ester; NCX-4040] (*para*-NO-ASA) were dissolved in DMSO to give stock solutions of 100 mmol/L. [2-(Acetyloxy)benzoic acid 3-[(nitrooxy)methyl]phenyl ester; NCX-4016] (*meta*-NO-ASA) was dissolved in DMSO to give a stock solution of 400 mmol/L. All drug stocks were aliquoted and stored at −20°C.

Treatment of cell lines with ASA and NO-ASA. To determine the IC_{50} of ASA and NO-ASA, cells were plated into either 12- or 24-well dishes at concentrations between 5 to 8×10^4 and 2.5 to 4×10^4 cells per well, respectively. Cells were treated with a selected range of concentrations of each ASA or NO-ASA drug; for example, 0.5, 1, 2.5, and 5 μmol/L of *ortho*-NO-ASA (see Supplementary Fig. S1). Negative controls of medium alone (DMEM) and DMEM + DMSO carrier (DMSO) were included in the analysis. The final concentration of DMSO in each cell treatment never exceeded 0.1%, except when final concentrations above 2 mmol/L of ASA were being examined. Drugs were added within a 3-h period after cells had been plated. Experiments were done in triplicate. After 5 days, cells were washed with PBS, trypsinized, pelleted at 1,000 rpm for 5 min, stained with 0.4% trypan blue, and viable cells were counted.

Long-term drug treatment for MSI analysis. Cells were initially plated into six-well dishes at 2×10^5 cells per well, and treated with ASA and NO-ASAs. The concentrations of ASA and NO-ASA were lower than the IC_{50}, and are found in Supplementary Tables S1 to S12. A smaller subset of two concentrations of each reagent was selected for long-term exposure of each cell line. Negative controls of DMEM and DMSO were included. Cells were split when confluent and were under continual exposure to the drugs. In the early stages of the treatments, cells were counted and re-plated at 2×10^5 cells per well. Exceptions were made if cells were growing poorly, usually as a consequence of drug treatment, and most often in the early days of the experiment. In this case, cells were split at a slightly higher density of 4 to 5×10^5 cells per well. At various time points, a portion of each cell suspension was saved for subsequent isolation of its genomic DNA and MSI analysis.

MSI analysis of treated cell line DNAs. The mouse primers used in this study have previously been reported by Kabbarah et al. (23) as TG_{27}, TA_{27}, GA_{29}, CT_{25}/CA_{27}, A_{33}, and T_{27}. They have been re-designated MSM01 to MSM06 herein for simplicity. The human primers have previously been reported by Ruschoff et al. (19) as BAT25, BAT26, BAT40, D5S346, D2S123, and D17S250. They have been re-designated MSM11 to MSM16 for simplicity. One oligomer of each primer set was 5′-labeled with FAM, VIC or NED. Details for all primer pairs are presented in Supplementary Table S13.

Genomic DNA was prepared from drug-treated mouse and human cell lines using a DNeasy tissue kit (Qiagen). DNA was amplified with Platinum Pfx DNA polymerase. The final components of the reaction mix were as follows: DNA (1–2 ng; ~ 100–200 genome equivalents; <0.5% total genomes); amplification buffer (2× concentration); 1 mmol/L of $MgSO_4$; 300 μmol/L of deoxynucleotide triphosphates; 300 nmol/L of each primer; 1 unit of Pfx; and H_2O to a final volume of 15 μL. The following amplification conditions were used as a standard: 94°C, 2 min (94°C, 30 s; 54°C, 30 s; 68°C, 30 s) for 30 to 35 cycles; 68°C, 2 min. Samples were diluted and analyzed on an Applied Biosystems 3730. At least three independent amplification reactions of each microsatellite sequence were examined for each genomic DNA sample.

Results

ASA and NO-ASA inhibit mammalian cell growth *in vitro*. Prior to treatment, we examined the effect of ASA and NO-ASA positional isomers on cell growth. Mammalian cell lines were seeded into 12- or 24-well plates at 2.5 to 5 $\times$ 10^4 cells/mL and treated with a range of ASA and NO-ASA concentrations. The IC_{50} values were determined following a 5-day exposure to estimate the appropriate drug concentrations that could be tolerated (Table 1). Representative survival curves are depicted in Supplementary Fig. S1.

The MMR-deficient murine colonocytes and MEFs appear to display a modest resistance to ASA and NO-ASA positional isomers compared with their isogenic wild-type controls (Table 1). For example, the *meta*-NO-ASA IC_{50} is 148 μmol/L for MMR-deficient $p53^{-/-}Msh2^{-/-}$ colonocytes, compared with 91 μmol/L for the corresponding MMR-proficient $p53^{-/-}$ colonocytes. These observations appear similar to the drug resistance observed when MMR-deficient cells are treated with several DNA damaging agents such as methylmethane sulfonate (for review, see ref. 24).

The human tumor cell line HCT116($hMLH1^{-/-}$) is MMR-deficient as a result of biallelic mutation of the *hMLH1* gene (22). Transfer of chromosome 2 or chromosome 3 into the HCT116($hMLH1^{-/-}$) cell line yielded the MMR-deficient HCT116($hMLH1^{-/-}$)+chr2($hMLH1^{-}$) cell line and the MMR-proficient HCT116($hMLH1^{-/-}$)+chr3($hMLH1^{+}$) cell line, respectively. The MMR status of these cell lines has been verified by repair assays and Western analysis for MLH1 expression (ref. 22; data not shown). These nearly isogenic human cell lines do not appear to show a consistent sensitivity to ASA or NO-ASA positional isomers. Although both cell lines lack hMLH1 and are MMR-deficient, the *meta*-NO-ASA IC_{50} is 138 μmol/L for HCT116($hMLH1^{-/-}$)+chr2($hMLH1^{-}$) but only 59 μmol/L for the parental cell line HCT116($hMLH1^{-/-}$). Similarly the *para*-NO-ASA IC_{50} is 2.29 μmol/L for HCT116($hMLH1^{-/-}$)+chr2($hMLH1^{-}$) and only 0.81 μmol/L for HCT116($hMLH1^{-/-}$). Restoration of MMR by expression of hMLH1 in the HCT116($hMLH1^{-/-}$)+chr3($hMLH1^{+}$) cell line confers increased tolerance to *meta*-NO-ASA compared with HCT116($hMLH1^{-/-}$). These data appear to underline the differences in human tumor cell line derivatives versus murine MEFs and colonocyte epithelial cells. Importantly, the murine cells were derived from isogenic mice that differ solely in their MMR (Msh2) status, whereas the tumor-derived human cell lines may harbor multiple known and unknown mutations associated with tumor development. The mechanism of modest resistance to ASA and NO-ASA positional isomers in $Msh2^{-/-}$ murine cell lines is unknown.

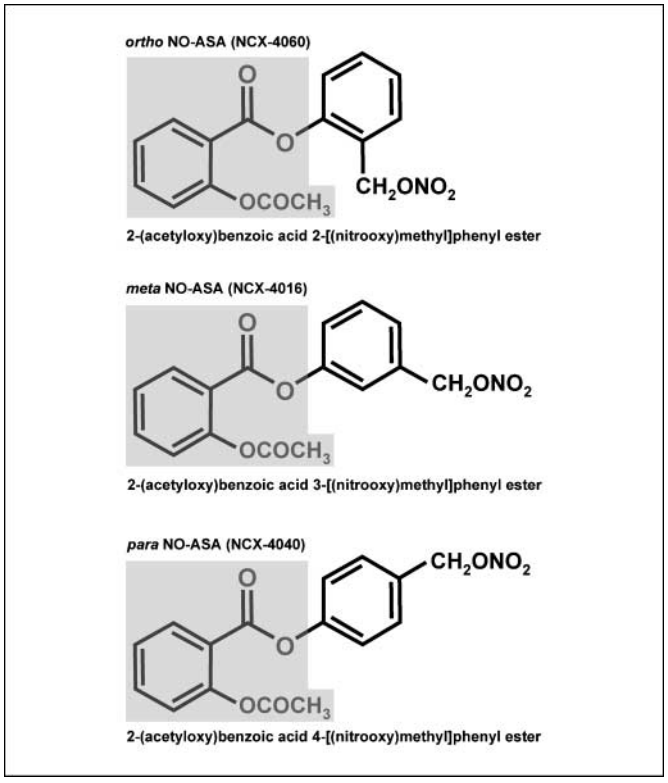

Figure 1. Structure of NO-ASA positional isomers. *ortho*-, *meta*-, and *para*-NO-ASA are an isomeric family of compounds based on the parental molecule of ASA (*gray box*). They differ only in the position at which the nitrogen-donating —CH_2ONO_2 group is attached to the benzene spacer.

Both the *ortho*-NO-ASA and *para*-NO-ASA isomers appear to be 500- to 4,000-fold more efficient than ASA at inhibiting mammalian cell growth (Table 1). The IC_{50} data highlights the striking effect that substitution of the —ONO_2 group at the *meta* position on the benzene linker has on the biological properties of this family of compounds (Fig. 1). The *meta*-NO-ASA seems to be 100- to 250-fold less efficient at inhibiting cell growth compared with the *ortho*- or *para*-NO-ASA. These results appear consistent with previous reports comparing these derivatives (2).

Development of a simplified screen for altered MSI. Previous work suggested that treatment of MMR-defective tumor cell lines with ASA or sulindac induced a genetic selection for microsatellite stability in MMR-defective human tumor cells (19). These studies were done by a laborious method that included isolation of multiple microclones from a total cell population during drug treatment. Once isolated, the microclones allowed the quantification of MSI within the population during the process of stabilization. For example, these studies suggested that numerous microclones isolated from hMSH2- and hMLH1-deficient tumor cell lines display 40% to 60% MSI. That is, 40% to 60% of the microclones differed in microsatellite size from a canonical starting size. Long-term treatment with ASA or sulindac resulted in <5% of these microclones with a different microsatellite size (19).

We reasoned that continuous splitting (reduction) of a population of growing cells undergoing selection for stable microsatellite sequences ($I^n \rightarrow S^{In}$) was the population equivalent of isolating stable microclones (Fig. 2*B*). This idea is based on the observation that ASA/sulindac–treated MSI cells were shown to enter an apoptotic pathway while the selected MSS cells continued to grow (19). Furthermore, sampling a fraction of the total genomes (<0.5% or $\sim$500 genome equivalents) at each time point enhanced the likelihood of identifying altered microsatellite sizes. By this method, we defined MSS when at least three independent fractional samples displayed an equivalent microsatellite pattern.

The final MSS cell population need not necessarily contain a single microsatellite size (S^{I1}). Rather the MSS cells might contain several microsatellite sizes (S^{In}) that would result in a combined MSS pattern (Fig. 2*B*). Our fractional genomic sampling method merely places a lower limit on the probability of cells in the population containing a recently altered microsatellite size that would result in classification as MSI.

Examples of the selection of an MSS cell population from an MSI cell population are shown in Fig. 2. Untreated E1A $Msh2^{-/-}$ MEFs display an enduring altered microsatellite pattern (MSI) relative to a known size control over the course of 156 days of growth: for these cells, this period approximates 156 generations (Fig. 2*A*). It

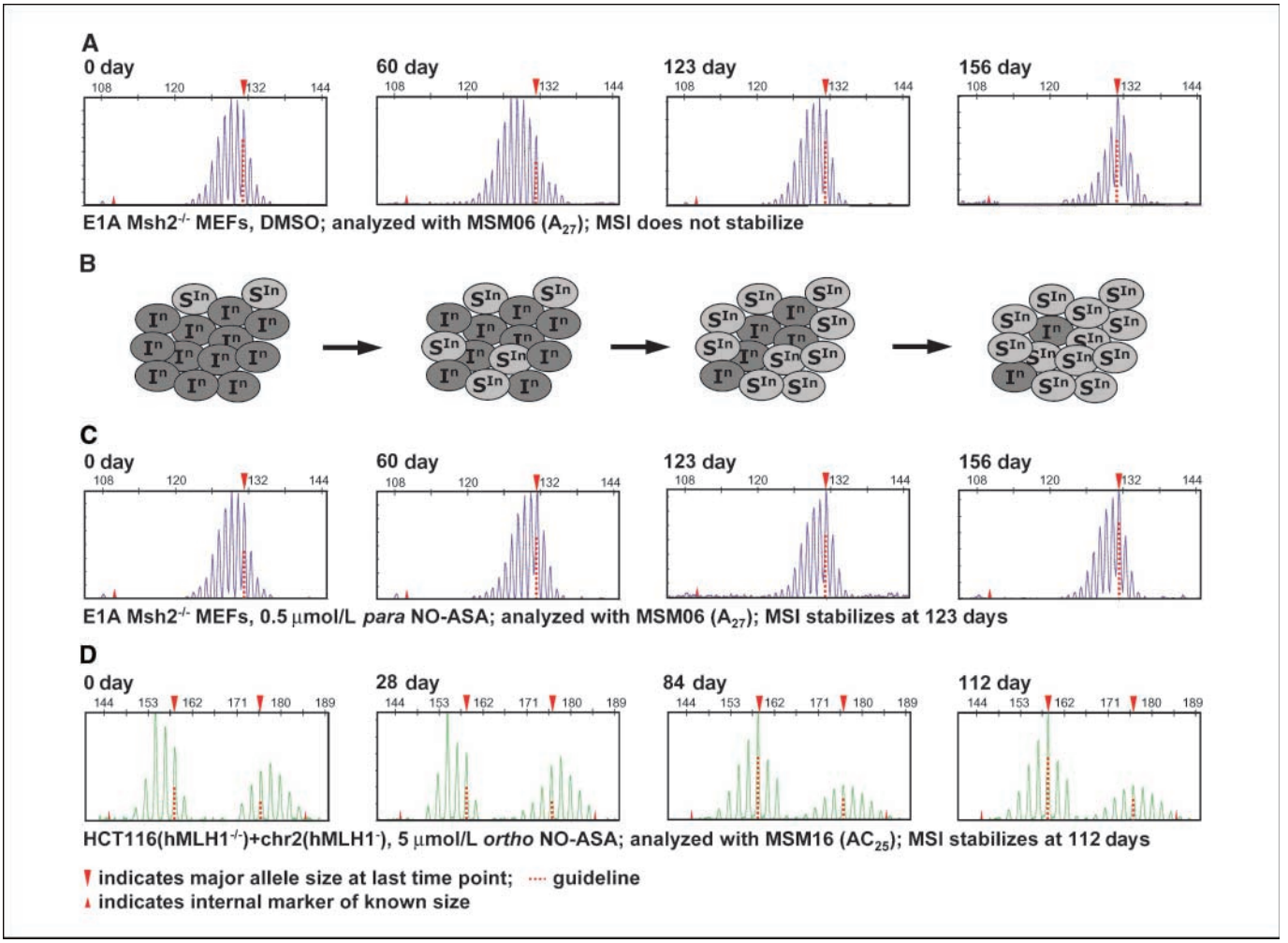

Figure 2. NO-ASA driven selection of MSS cells from a founding population of genetically microsatellite unstable cells. *A,* the MSI profile of untreated E1A $Msh^{-/-}$ MEFs continues to change in culture over time. Because there is no drug treatment, there is no selection process for an emergent stable microsatellite profile. The MSI profile of this cell line, as assessed by amplification of MSM06 (A_{27}), is different at all of the sample times, indicating continuing instability of the mean allele size of this locus. *B,* the MSI/MSS screen suggests that within the microsatellite-unstable population of MMR-defective cells containing *n* microsatellite lengths (*dark gray circles;* I^n, Instability), there is a subset of cells that have a MSS phenotype with a subset of S^{In} microsatellite lengths, (*light gray circles;* S^{In}, Stabilization of Instability). Although the latter cells only comprise a minority of the total cell population, they can be selected by treatment with NO-ASAs (see ref. 19). These agents confer either a subsequent growth advantage to cells that are S^{In} and/or selectively eliminate cells that are I^n, through apoptotic processes (19). With continual exposure to NO-ASAs, the relative proportion of S^{In} cells within the population increases to the point where they eclipse the I^n cells. Note that emergent S^{In} cells do not necessarily have the same stable microsatellite pattern (i.e., they are only required to retain a stable phenotype). *C,* E1A $MSH^{-/-}$ MEFs treated with *para*-NO-ASA demonstrate stabilization of MSI at marker MSM06 (A_{27}). Prolonged exposure results in stabilization of the MSI profile after 123 days (compare 123 days to 156 days). *D,* HCT116(hMLH1$^{-/-}$)+chr2(hMLH1$^-$) cells treated with *ortho*-NO-ASA demonstrate stabilization of MSI at microsatellite marker MSM16 (AC_{25}). The MSM16 marker contains two alleles. Although single-allele stabilization appears to have occurred by 84 days, drug-induced stabilization of both alleles by treatment with *ortho*-NO-ASA occurred only by 112 days (see Fig. 5). *Small arrowhead,* position of known size control (*bottom*); *large arrowhead* and *dashed line,* position of major allele(s) relative to the last time point (*top*).

should be noted that the amplification of microsatellite sequences by PCR results in a normal distribution of repeat sizes surrounding the absolute microsatellite size (stutter pattern). The available data suggests that this is a result of repetitive polymerase misincorporation errors associated with cyclic (PCR) copying of repeat sequences (25). The absolute length of a microsatellite may be determined as the highest peak length within the stutter pattern. For a population of cells with multiple microsatellite lengths, the highest peak length within the stutter pattern corresponds to the average microsatellite size.

In contrast to untreated cells, E1A $Msh2^{-/-}$ MEFs treated continuously with 0.5 μmol/L of *para*-NO-ASA display MSI that gradually transitions to a stable microsatellite size pattern (MSS) by 123 days (Fig. 2*C*). Similarly, HCT116(hMLH1$^{-/-}$)+chr2(hMLH1$^-$) treated with 5 μmol/L of *ortho*-NO-ASA displayed MSI at heterozygous microsatellite alleles of a single locus (Fig. 2*D*). However, by 112 days of continuous treatment, both alleles display MSS (Fig. 2*D*). This analysis of altered/stable microsatellite patterns was used to screen mouse and human MMR-deficient cell lines using panels of six mouse or six human diagnostic microsatellite markers, respectively (Supplementary Table S13).

ASA and NO-ASA treatment regimen for mammalian cell lines. The IC_{50} data (Table 1) was instrumental in estimating the concentrations of ASA and NO-ASAs to be used for the long-term exposure of mouse E1A MEFs and colonocytes. A range of drug concentrations roughly centered on the IC_{50} values was initially selected. We regarded it likely that drug concentrations much higher than the IC_{50} would result in population cell death, especially

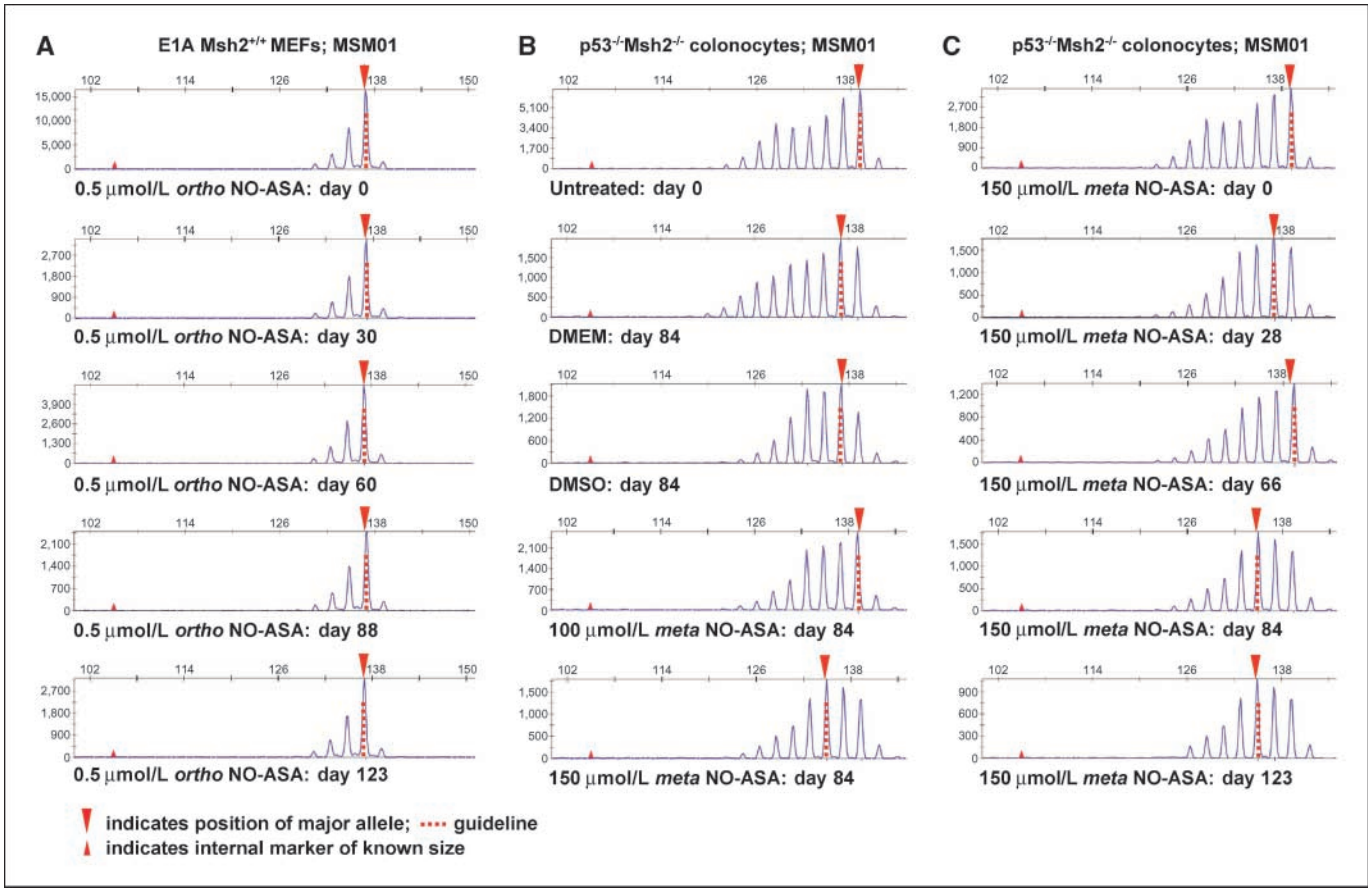

Figure 3. Long-term treatment of MMR-deficient mouse cell lines with NO-ASAs selects for a population of MSS cells. *A,* treatment of MSS E1A $Msh2^{+/+}$ MEFs with NO-ASAs does not alter the microsatellite marker pattern. MMR-proficient E1A $Msh2^{+/+}$ MEFs were split at day 0 and subjected to treatment with 0.5 μmol/L of *ortho*-NO-ASA. DNA samples were prepared from cells at the times indicated and marker MSM01 was analyzed to reveal any drug-induced changes of this microsatellite pattern (see Supplementary Tables S1–S8). *B,* the MSI status of $p53^{-/-}Msh2^{-/-}$ colonocytes indicates independent evolution of microsatellite patterns following different treatments of the same starting cell line. MMR-defective colonocytes were split at day 0 and subjected to the treatments shown. After 84 days, all cell lines displayed a different pattern for microsatellite marker MSM01 compared with $t = 0$; major allele bands of 137, 137, 139, and 135 bp, respectively (*top* to *bottom*). *C,* treatment of $p53^{-/-}Msh2^{-/-}$ colonocytes with *meta*-NO-ASA selects for a cell population that displays a stable microsatellite pattern at the previously unstable microsatellite marker MSM01. MMR-defective mouse colonocytes were treated with *meta*-NO-ASA and DNA samples were isolated at the times indicated. After 28 days, the major allele was 137 bp, which had changed to 139 bp by day 66, and then 135 bp by day 84. At day 123 and all-subsequent days, MSM01 remained constant at 135 bp, indicating that drug treatment had resulted in stabilization at this previously unstable microsatellite marker. *Small arrowheads,* positions of known size control (*bottom*); *large arrowhead* and *dashed line,* positions of major allele (*top*).

during long-term exposure. However, it was formally possible that such long-term exposure might result in drug tolerance and eventual adaptation of these cell lines to increased concentrations of the NO-ASAs.

We found E1A $Msh2^{+/+}$ MEFs to be most sensitive to the growth-inhibitory effects of the NO-ASAs. Maintenance of these cells in medium containing 1 and 2.5 μmol/L of either *ortho*-NO-ASA or *para*-NO-ASA resulted in complete cell death in 67 and 33 days, respectively (data not shown). Moreover, cells could not be successfully nurtured beyond these time points regardless of altered seeding densities. In contrast, the HCT116-derived cell lines appeared to thrive during prolonged treatment with *ortho*-NO-ASA and *para*-NO-ASA concentrations above their 5-day IC_{50} values. We found that it was possible to maintain and propagate these lines in 5 μmol/L of either *ortho*- or *para*-NO-ASA. Although an initial lag in cell growth was observed, the HCT116-derived cells recovered and displayed normal growth kinetics by 2 weeks of culture and were viable for the duration of the study. The basis of this limited drug tolerance is unknown and might be related to their tumor cell characteristics. This observation underlines the importance of examining relatively normal isogenic mammalian cell lines in comparison to tumor-derived cell lines.

Figure 4. Long-term treatment of MMR-deficient human HNPCC cell lines with NO-ASAs selects for a population of MSS cells. *A* and *B,* MSS HCT116($hMLH1^{-/-}$)+ch3($hMLH^{+}$) cells are unaffected by long-term treatment with NO-ASAs. MMR-proficient HCT116($hMLH1^{-/-}$)+ch3($hMLH^{+}$) cells were subjected to treatment with 5 μmol/L of *ortho*-NO-ASA. DNA was isolated from cells at the times indicated and amplified with (*A*) marker MSM16 (AC_{25}) and (*B*) marker MSM13 (T_{40}). *C* and *D,* treatment of HCT116($hMLH1^{-/-}$) cells with *ortho*-NO-ASA results in selection for a cell population that displays stabilization at previously unstable microsatellite markers. HCT116($hMLH1^{-/-}$) cells are MMR-deficient and are MSI. *C,* treatment with 5 μmol/L of *ortho*-NO-ASA changes the mean allele size of marker MSM15 (AC_{28}) from 213 to 211 bp by day 112. This shift in allele size becomes stable and does not change upon further duration of treatment. *D,* treatment with 5 μmol/L of *ortho*-NO-ASA changes the mean allele sizes of marker MSM14 (AC_{14}). The MSM14 marker contains two alleles, which achieve stabilization independently of each other. The smaller allele stabilizes at 106 bp by day 84, whereas the larger allele stabilized at 116 bp by day 112. *Small arrowheads,* positions of known size control (*bottom*); *large arrowhead* and *dashed line,* positions of major alleles (*top*).

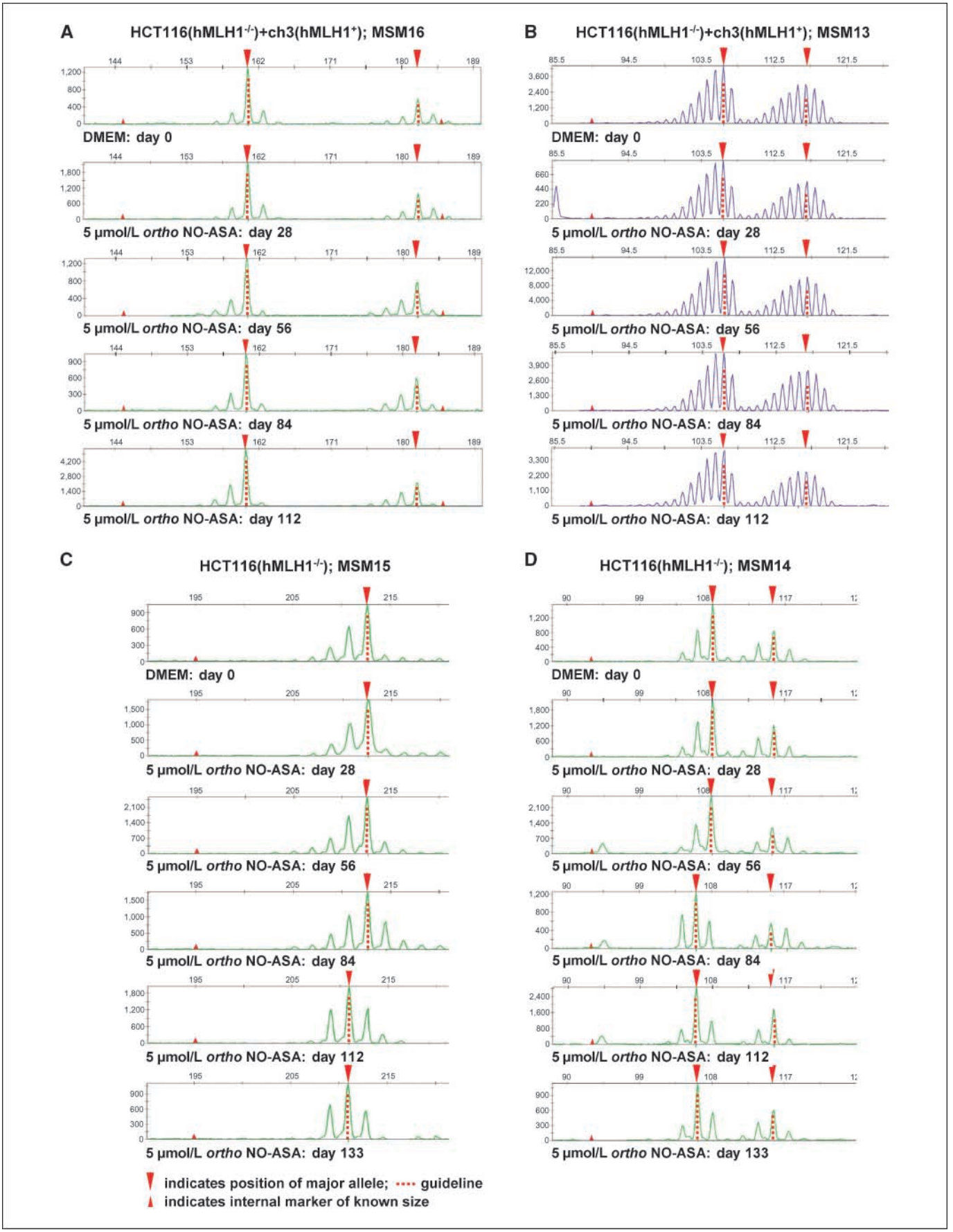
A
HCT116(hMLH1-/-)+ch3(hMLH1+); MSM16
DMEM: day 0
5 μmol/L ortho NO-ASA: day 28
5 μmol/L ortho NO-ASA: day 56
5 μmol/L ortho NO-ASA: day 84
5 μmol/L ortho NO-ASA: day 112
B
HCT116(hMLH1-/-)+ch3(hMLH1+); MSM13
DMEM: day 0
5 μmol/L ortho NO-ASA: day 28
5 μmol/L ortho NO-ASA: day 56
5 μmol/L ortho NO-ASA: day 84
5 μmol/L ortho NO-ASA: day 112
C
HCT116(hMLH1-/-); MSM15
DMEM: day 0
5 μmol/L ortho NO-ASA: day 28
5 μmol/L ortho NO-ASA: day 56
5 μmol/L ortho NO-ASA: day 84
5 μmol/L ortho NO-ASA: day 112
5 μmol/L ortho NO-ASA: day 133
D
HCT116(hMLH1-/-); MSM14
DMEM: day 0
5 μmol/L ortho NO-ASA: day 28
5 μmol/L ortho NO-ASA: day 56
5 μmol/L ortho NO-ASA: day 84
5 μmol/L ortho NO-ASA: day 112
5 μmol/L ortho NO-ASA: day 133
indicates position of major allele; guideline
indicates internal marker of known size

Prolonged exposure of mammalian cell lines to ASA and NO-ASA. We treated the murine cell lines with 0.5 and 1.5 mmol/L of ASA, 0.1 and 0.5 μmol/L of *ortho*-NO-ASA, 100 and 150 μmol/L of *meta*-NO-ASA, and 0.1 and 0.5 μmol/L of *para*-NO-ASA. The only exception to this treatment regime were E1A Msh2$^{+/+}$ MEFs, which were treated with 0.1 and 0.25 mmol/L of ASA because they proved comparatively more sensitive to this compound than the other cell lines. The cell lines were split at the onset of the study, considered as day 0 (t = 0), and subjected to continual long-term cultivation. Negative controls included cell culture in medium alone (DMEM) and cell culture in medium plus DMSO. After t = 0, each treatment was considered to generate separate cell lines which were analyzed individually with six microsatellite markers (see Materials and Methods).

Cell lines were treated with ASA and NO-ASAs for up to 156 days. Complete MSI/MSS data for each cell line is tabulated in Supplementary Tables S1 to S8. A central premise was that NO-ASA treatment would uniquely affect the microsatellite patterns of MMR-deficient cells but not MMR-proficient cells. This prediction was substantiated by the observation that these compounds did not alter the microsatellite size pattern(s) of any of the MMR-proficient cells examined (Fig. 3*A*; Supplementary Tables S1–S8).

MSI analysis suggested that the MMR-deficient murine cell lines continue to independently evolve novel microsatellite size patterns. For example, examination of p53$^{-/-}$Msh2$^{-/-}$ colonocytes at 84 days following growth in DMEM, DMSO, 100 μmol/L of *meta*-NO-ASA, and 150 μmol/L of *meta*-NO-ASA results in four different MSI profiles for marker MSM01 (Fig. 3*B*). These cell lines originated from a single parental cell line (day 0) that was then split and subjected to the drug regimes. At 84 days posttreatment, the microsatellite size patterns of all the cell lines appeared different (Fig. 3*B*). These data strongly suggest independent evolution of MSI cells.

An example of p53$^{-/-}$Msh2$^{-/-}$ colonocyte microsatellite sequence (MSM01) analysis over the course of treatment with 150 μmol/L of *meta*-NO-ASA is shown in Fig. 3*C*. The microsatellite size pattern appears altered relative to its preceding pattern until day 123. At day 123, the microsatellite size pattern appears identical to day 84. All succeeding and redundant analyses of this microsatellite repeat sequence from these p53$^{-/-}$Msh2$^{-/-}$ colonocytes treated with 150 μmol/L of *meta*-NO-ASA appeared identical to day 84 (data not shown). These results are consistent with the conclusion that long-term treatment of p53$^{-/-}$Msh2$^{-/-}$ colonocytes with 150 mmol/L of *meta*-NO-ASA induced MSS for the MSM01 microsatellite.

The initial microsatellite size profiles of HCT116(hMLH1$^{-/-}$), HCT116(hMLH1$^{-/-}$)+chr2(hMLH1^{-}), and HCT116(hMLH1$^{-/-}$)+chr3-(hMLH1^{+}) cell lines for the six diagnostic microsatellite markers suggests that these cell lines are not absolutely isogenic (Supplementary Fig. S2). However, numerous studies have detailed the complementation and apparent full function of hMLH1 in the HCT116(hMLH1$^{-/-}$)+chr3(hMLH1^{+}) cell line (22, 26). We observed differences between these three cell lines in both major allele size and the PCR stutter pattern for MSM12, MSM13, and MSM16 (Supplementary Fig. S2). This observation is best exemplified by the MSM13 microsatellite. The HCT116(hMLH1$^{-/-}$) tumor cell line contained two major allele sizes of 106 and 116 bp. These sizes should be considered relative to the consensus allele size in most normal human tissues of 126 bp (27). This result is consistent with the general observation of shortened allele sizes in most MSI human tumors as well as the original HCT116(hMLH1$^{-/-}$) MSI tumor cell line (17, 28). The construction of the HCT116-(hMLH1$^{-/-}$)+chr2(hMLH1^{-}) and HCT116(hMLH1$^{-/-}$)+chr3-(hMLH1^{+}) cell lines resulted in the isolation of clones from the original HCT116(hMLH1$^{-/-}$) parent line with additional microsatellite size differences. These included 103 and 117 bp in the HCT116(hMLH1$^{-/-}$)+chr2(hMLH1^{-}) cell line as well as 105 and 115 bp in the HCT116(hMLH1$^{-/-}$)+chr3(hMLH1^{+}) cell line (Supplementary Fig. S2). The stutter pattern also revealed qualitative differences between these cell lines.

The microsatellite size patterns of the MMR-proficient HCT116(hMLH1$^{-/-}$)+chr3(hMLH1^{+}) cell line were stable and unaltered compared with the starting microsatellite size pattern following treatment with ASA or NO-ASAs (Fig. 4*A* and *B*; see Supplementary Tables S9–S12). These results are quantitatively similar to the MMR-proficient mouse cell lines (Fig. 3; Supplementary Tables S1–S8). Examples of microsatellite size stabilization following treatment of the MMR-deficient HCT116(hMLH1$^{-/-}$) cell line with *ortho*-NO-ASA are shown in Fig. 4*C* and *D*. We noted the stabilization of the *MSM15* allele at 211 bp by day 112 (Fig. 4*C*). Similarly, we noted the stabilization of the small *MSM14* allele at 106 bp by day 84 and the large allele at 116 bp by day 112 (Fig. 4*D*). These results suggest that ASA- and NO-ASA–dependent stabilization of MSI is allele-specific, even within a single microsatellite. We scored drug-induced MSS only when both alleles displayed stability.

Treatment of MMR-deficient cells with ASA and NO-ASA results in dose-dependent microsatellite stability. A complete analysis of long-term ASA and NO-ASA exposure using the panel of six mouse/human-specific microsatellite sequences was performed with the E1A MEFs and p53$^{-/-}$Msh2$^{-/-}$ colonocytes (Fig. 5*A* and *B*; Supplementary Tables S1–8) and the HCT116-derived human tumor cell lines (Fig. 5*C* and *D*; Supplementary Tables S9–S12). The data are displayed in a bar format to allow an overall view of microsatellite marker stability compared with untreated controls and the MMR-proficient control cell lines. We found that treatment of the MMR-deficient cell lines with ASA and NO-ASA resulted in a dose-dependent MSS of normally unstable microsatellite markers (Fig. 5). The greatest stabilization following any treatment regime was four of six microsatellite markers (67%). Dinucleotide microsatellite repeat sequences seemed to display ASA- and NO-ASA–induced MSS to a greater extent and at earlier time points than mononucleotide microsatellite repeat sequences. These latter results seemed consistent with the observation that mononucleotide microsatellite repeat sequences were more prone to MSI even in marginally MMR-deficient genetic backgrounds (23, 29, 30).

Treatment of the E1A Msh2$^{-/-}$ MEFs and p53$^{-/-}$Msh2$^{-/-}$ colonocytes with 0.5 μmol/L of *ortho*-NO-ASA resulted in a residual MSI of 33% (two of six) which borders on the National Cancer Institute–recommended diagnosis of MSI (Fig. 5*A* and *B, lane 4*; ref. 17) and is below the diagnosis of MSI derived from a large-scale survey of microsatellite markers (28). There appeared to be no consistent time of onset of the dose-dependent MSS of MMR-deficient cell lines. However, the earliest onset of MSS of a single microsatellite marker occurred at 60 days posttreatment of the E1A Msh2$^{-/-}$ MEFs with ASA (0.5 and 1.5 mmol/L) and *ortho*-NO-ASA (0.5 μmol/L), the p53$^{-/-}$Msh2$^{-/-}$ colonocytes with 0.1 μmol/L of *para*-NO-ASA, and the HCT116(hMLH1$^{-/-}$)+chr2(hMLH1^{-}) with 5.0 μmol/L of *para*-NO-ASA. Because these cell lines, on average, displayed a 24-h doubling time, the number of generations required to develop MSS appears nearly equivalent to the number of days posttreatment. The relative suppression of MSI by ASA and

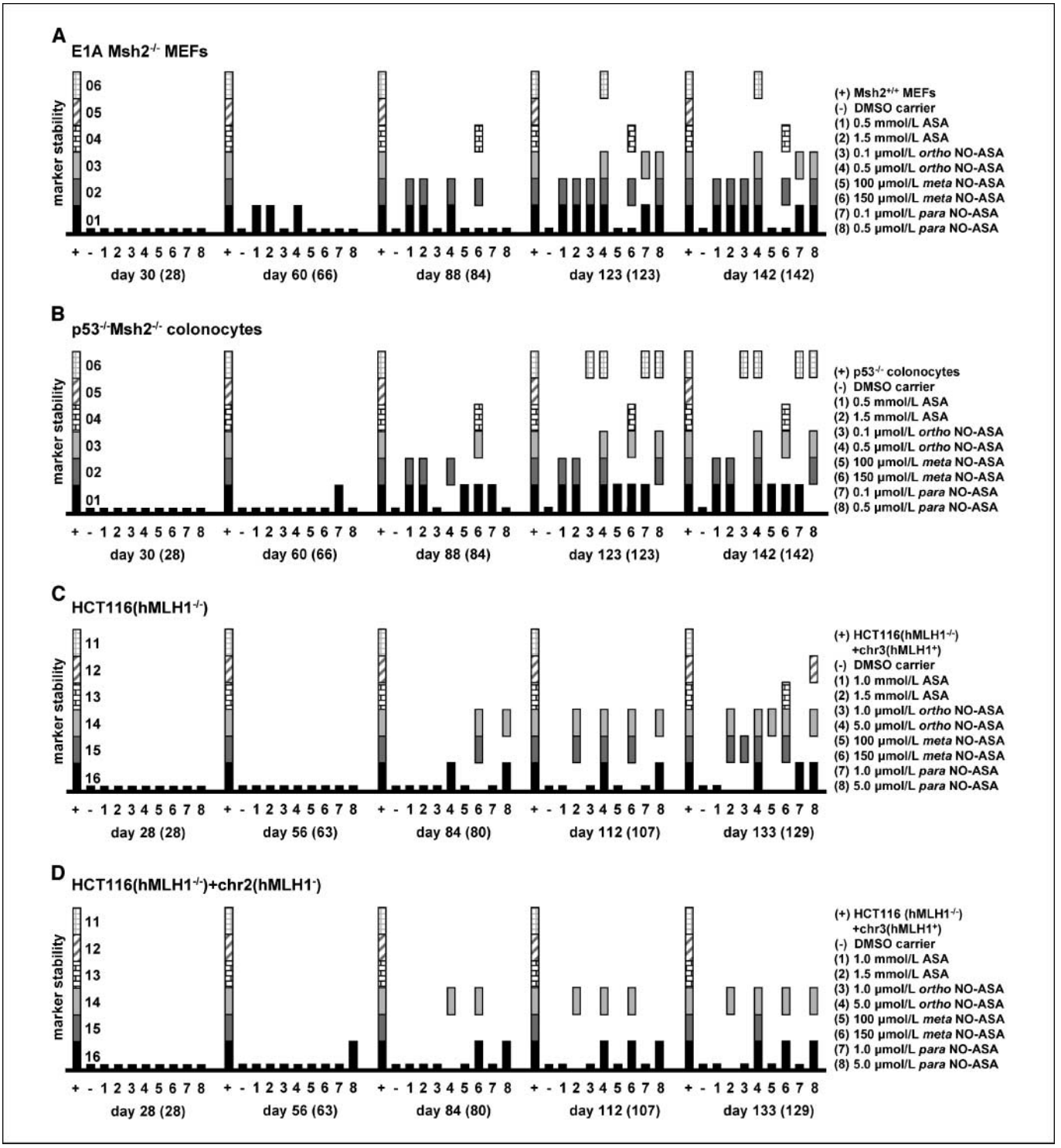

Figure 5. Dose-dependent stabilization of MSI in MMR-deficient cell lines following prolonged treatment with ASA and NO-ASA. Changes in microsatellite patterns were assessed with six microsatellite markers for both the murine (MSM01–06) and human (MSM11–16) cell lines; designated 01-06 (TG_{27}, TA_{27}, GA_{29}, CT_{25}/CA_{27}, A_{33}, T_{27}) and 11-16 (T_{26}, A_{26}, T_{40}, AC_{14}, AC_{28}, AC_{25}), respectively, as indicated on far left *Y*-axis (see Supplementary Table S13). Changes that result in microsatellite stability of these selected markers following long-term exposure to ASA and NO-ASAs are shown as six arbitrarily shaded bars, indicating the observed stability of individual microsatellites. The positive controls (+) for each panel are the respective MMR-proficient cell lines: *A,* E1A $Msh2^{+/+}$ MEFs; *B,* $p53^{-/-}$ colonocytes; *C,* HCT116($hMLH1^{-/-}$)+chr3($hMLH^{+}$); *D,* HCT116($hMLH1^{-/-}$)+chr3($hMLH^{+}$). These MMR-proficient cell lines are represented by six bars, demonstrating the complete stability of each microsatellite studied, which remains unaltered with treatment (see Fig. 3). Conversely, the negative controls (−) represent the comparable isogenic MMR-deficient cell lines treated with DMSO only: *A,* E1A $Msh2^{-/-}$ MEFs; *B,* $p53^{-/-}Msh2^{-/-}$ colonocytes; *C,* HCT116($hMLH1^{-/-}$); *D,* HCT116($hMLH1^{-/-}$)+chr2($hMLH1^{-}$). These cell lines lack a representative bar for any of the microsatellite markers, indicating fundamental MSI that remains unaltered over time. The treatment parameters of the MMR-deficient cell lines are keyed to the numbers on the far right *Y*-axis and correspond to the numbers above each treatment day. For example, in *A,* E1A $Msh2^{-/-}$ MEFs treated with 0.5 mol/L (1) and 1.5 mol/L (2) of ASA display stabilization at marker MSM01 (*bottom, black bars*) at day 60. At day 88, marker MSM02 (*second, medium gray bar*), in addition to MSM01 also displays stabilization. These summarized bar data are derived from Supplementary Tables S1–12. Numbers in parenthesis on the *X*-axis represent the time points at which data for *meta*-NO-ASA were obtained.

NO-ASA derivatives did not seem to be equivalent when cell lines were compared (Fig. 5). However, taken as a whole, our data are consistent with the conclusion that treatment of MMR-deficient cells with ASA and NO-ASA leads to widespread dose-dependent suppression of MSI. These results are qualitatively similar to previous studies of ASA- and sulindac-treated human tumor cell lines (19).

Discussion

We have demonstrated that continuous long-term exposure of genetically defined MMR-deficient murine and human HNPCC cell lines to ASA and NO-ASA positional isomers resulted in a dose-dependent widespread suppression of MSI. The level of this suppression is incomplete. However, in all cases, a minimum of 50% of the diagnostic microsatellite markers appear to be stabilized by at least one of the NO-ASA positional isomers. Dinucleotide microsatellite markers seem to be preferentially stabilized compared with mononucleotide microsatellite markers. These latter results appear consistent with genetic and biochemical studies that have shown a preference for mononucleotide repeat instability in cells with marginal MSI and suggests that replication fidelity may underpin the selection of MSS cells.

MMR gene defects that have been clearly linked to widespread MSI include *hMSH2, hMSH6, hMLH1,* and *hPMS2* (*hMLH3* remains controversial; ref. 16). Alteration of any of these genes affects the stability of mononucleotide, dinucleotide, and complex microsatellite sequences as well as base substitution mutations. Because there has been no reported dissociation of MSI from base substitution mutagenesis, we regard it likely that suppression of MSI by ASA and NO-ASA would also result in suppression of the widespread mutator phenotype (base substitution mutagenesis) associated with cellular MMR defects.

Although previous studies have implicated apoptosis in ASA selection of MSS in MMR-deficient HNPCC cells (19), the mechanism of the NO-ASA positional isomer–selective process for MSS is unknown. A detailed understanding of the components associated with the induced apoptotic selection by ASA and its functional derivatives remains enigmatic. Moreover, it is unclear whether MSI suppression depends uniquely on the ASA moiety or is enhanced by the NO-donating group. Because the suppression of MSS occurs in genetic backgrounds that are deficient in hMSH2–hMSH6 or hMLH1–hPMS2, the role of ASA and NO-ASA in MSS selection must *a priori* be independent of these protein complexes. Moreover, because there seems to be little change in doubling times of the treated and untreated cells, it would be unlikely that differential growth suppression could be a significant contributor to the selective process. The existing data seems to suggest that ASA and NO-ASA lowers the threshold for cellular damage–induced apoptosis such that it includes postreplication mismatched nucleotides. Because the normal mismatch detection system is defective, sensing these lesions seems to occur independently of the fundamental MMR components. However, we have not ruled out the possibility that suppression of MSI might include components of the MMR-dependent damage-induced apoptosis signaling pathway.

The murine cell lines used in this study contain deleted or attenuated p53. In fact, the only methodology to date for the consistent isolation of murine colonocyte epithelial cells requires genetic deletion of p53 from the starting tissues (31). However, the HCT116-derived human cell lines contain wild-type p53 and have been consistently used for studies involving normal p53 function(s). Because our results seem to be constant across several mammalian cell lines with varying p53 status, we regard it unlikely that p53 plays a significant role in the suppression of MSI or the mechanism that leads to this suppression. However, we cannot rule out a competing role for p53 in the ASA/NO-ASA apoptotic selective process because there seems to be modestly less suppression of MSI in the HCT116-derived cell lines ($p53^+$) compared with the murine cell lines ($p53^-$). The suppression of MSI by ASA and NO-ASA positional isomers in fibroblasts, colonic epithelial cells, and tumor cells suggests that the suppression components and/or mechanism(s) are largely conserved across many cell types.

We find a consistent hierarchy in the suppression of MSI by these ASA derivatives: *ortho*-NO-ASA $\approx$ *para*-NO-ASA > *meta*-NO-ASA $\gg$ ASA. The doses required for the *ortho*-NO-ASA and *para*-NO-ASA to suppress MSI seem to be 10- to 100-fold less than *meta*-NO-ASA and 300- to 3,000-fold less than ASA. Such reduced doses may significantly attenuate the clinically relevant side effects associated with ASA and sulindac. The combination of enhanced suppression of MSI at significantly reduced dosages suggests that the *ortho*- and *para*-NO-ASA derivatives may be useful chemopreventives for carriers of the MMR deficiency associated with HNPCC.

Acknowledgments

Received 7/9/2007; revised 8/17/2007; accepted 9/21/2007.

Grant support: NCI grants CA67007 and CN-43302.

The costs of publication of this article were defrayed in part by the payment of page charges. This article must therefore be hereby marked *advertisement* in accordance with 18 U.S.C. Section 1734 solely to indicate this fact.

We thank Cinzia Sevignani for helpful discussions and expert advice, Tina Bocker for advice on MSI analysis, Hannes Alder for oligonucleotides and sequencing analyses, and Kristine Yoder for discussion and editorial advice.

References

1. Thun MJ, Henley SJ, Patrono C. Nonsteroidal anti-inflammatory drugs as anticancer agents: mechanistic, pharmacologic, and clinical issues. J Natl Cancer Inst 2002;94:252–66.
2. Rigas B, Kashfi K. Nitric-oxide-donating NSAIDs as agents for cancer prevention. Trends Mol Med 2004;10:324–30.
3. Kashfi K, Ryan Y, Qiao LL, et al. Nitric oxide-donating nonsteroidal anti-inflammatory drugs inhibit the growth of various cultured human cancer cells: evidence of a tissue type-independent effect. J Pharmacol Exp Ther 2002;303:1273–82.
4. Williams JL, Nath N, Chen J, et al. Growth inhibition of human colon cancer cells by nitric oxide (NO)-donating aspirin is associated with cyclooxygenase-2 induction and β-catenin/T-cell factor signaling, nuclear factor-κB, and NO synthase 2 inhibition: implications for chemoprevention. Cancer Res 2003;63:7613–8.
5. Yeh RK, Chen J, Williams JL, et al. NO-donating nonsteroidal antiinflammatory drugs (NSAIDs) inhibit colon cancer cell growth more potently than traditional NSAIDs: a general pharmacological property? Biochem Pharmacol 2004;67:2197–205.
6. Kaza CS, Kashfi K, Rigas B. Colon cancer prevention with NO-releasing NSAIDs. Prostaglandins Other Lipid Mediat 2002;67:107–20.
7. Rigas B, Kashfi K. Cancer prevention: a new era beyond cyclooxygenase-2. J Pharmacol Exp Ther 2005;314:1–8.
8. Bak AW, McKnight W, Li P, et al. Cyclooxygenase-independent chemoprevention with an aspirin derivative in a rat model of colonic adenocarcinoma. Life Sci 1998;62:PL367–73.
9. Williams JL, Kashfi K, Ouyang N, del Soldato P, Kopelovich L, Rigas B. NO-donating aspirin inhibits intestinal carcinogenesis in Min (APC(Min/+)) mice. Biochem Biophys Res Commun 2004;313:784–8.
10. Rao CV, Reddy BS, Steele VE, et al. Nitric oxide-releasing aspirin and indomethacin are potent inhibitors against colon cancer in azoxymethane-treated rats:

effects on molecular targets. Mol Cancer Ther 2006;5:1530–8.
11. Ouyang N, Williams JL, Tsioulias GJ, et al. Nitric oxide-donating aspirin prevents pancreatic cancer in a hamster tumor model. Cancer Res 2006;66:4503–11.
12. Fiorucci S, Santucci L, Gresele P, Faccino RM, Del Soldato P, Morelli A. Gastrointestinal safety of NO-aspirin (NCX-4016) in healthy human volunteers: a proof of concept endoscopic study. Gastroenterology 2003;124:600–7.
13. Iyer RR, Pluciennik A, Burdett V, Modrich PL. DNA mismatch repair: functions and mechanisms. Chem Rev 2006;106:302–23.
14. Fishel R, Acharya S, Berardini M, et al. Signaling mismatch repair: the mechanics of an adenosine-nucleotide molecular switch. Cold Spring Harbor Symp Quant Biol 2000;65:217–24.
15. Peltomaki P. Lynch syndrome genes. Fam Cancer 2005;4:227–32.
16. Boland CR, Fishel R. Lynch syndrome: form, function, proteins, and basketball. Gastroenterology 2005;129:751–5.
17. Boland CR, Thibodeau SN, Hamilton SR, et al. A National Cancer Institute Workshop on Microsatellite Instability for cancer detection and familial predisposition: development of international criteria for the determination of microsatellite instability in colorectal cancer. [Review, 119 refs]. Cancer Res 1998;58:5248–57.
18. Loeb LA. Mutator phenotype may be required for multistage carcinogenesis. Cancer Res 1991;51:3075–9.
19. Ruschoff J, Wallinger S, Dietmaier W, et al. Aspirin suppresses the mutator phenotype associated with hereditary nonpolyposis colorectal cancer by genetic selection. Proc Natl Acad Sci U S A 1998;95:11301–6.
20. McCurrach ME, Lowe SW. Methods for studying pro- and antiapoptotic genes in nonimmortal cells. Methods Cell Biol 2001;66:197–227.
21. Sevignani C, Cranston A, Iozzo RV, Fishel R, Calabretta B. Spontaneous and mutagen-induced transformation of primary cultures of $Msh2^{-/-}p53^{-/-}$ colonocytes. Cancer Res 1999;59:5882–6.
22. Koi M, Umar A, Chauhan DP, et al. Human chromosome 3 corrects mismatch repair deficiency and microsatellite instability and reduces *N*-methyl-*N*′-nitro-*N*-nitrosoguanidine tolerance in colon tumor cells with homozygous hMLH1 mutation. Cancer Res 1994;54:4308–12.
23. Kabbarah O, Mallon MA, Pfeifer JD, Edelmann W, Kucherlapati R, Goodfellow PJ. A panel of repeat markers for detection of microsatellite instability in murine tumors. Mol Carcinog 2003;38:155–9.
24. Karran P. Mechanisms of tolerance to DNA damaging therapeutic drugs. Carcinogenesis 2001;22:1931–7.
25. Streisinger G, Owen J. Mechanisms of spontaneous and induced frameshift mutation in bacteriophage T4. Genetics 1985;109:633–59.
26. Meyers M, Theodosiou M, Acharya S, et al. Cell cycle regulation of the human DNA mismatch repair genes hMSH2, hMLH1, and hPMS2. Cancer Res 1997;57:206–8.
27. Umar A, Boland CR, Terdiman JP, et al. Revised Bethesda Guidelines for hereditary nonpolyposis colorectal cancer (Lynch syndrome) and microsatellite instability. J Natl Cancer Inst 2004;96:261–8.
28. Dietmaier W, Wallinger S, Bocker T, Kullmann F, Fishel R, Ruschoff J. Diagnostic microsatellite instability: definition and correlation with mismatch repair protein expression. Cancer Res 1997;57:4749–56.
29. Papadopoulos N, Nicolaides NC, Liu B, et al. Mutations of GTBP in genetically unstable cells. Science 1995;268:1915–7.
30. Wei K, Clark AB, Wong E, et al. Inactivation of exonuclease 1 in mice results in DNA mismatch repair defects, increased cancer susceptibility, and male and female sterility. Genes Dev 2003;17:603–14.
31. Sevignani C, Wlodarski P, Kirillova J, et al. Tumorigenic conversion of p53-deficient colon epithelial cells by an activated Ki-ras gene. J Clin Invest 1998;101:1572–80.